Structures 64 (2024) 106521

Contents lists available at ScienceDirect

Structures

journal homepage: www.elsevier.com/locate/structures

Bolt load looseness detection for slip-critical blind bolt based on wavelet analysis and deep learning

Xing Gao [a,b], Wei Wang [a,b,*], Jiajun Du [a,b]

[a] State Key Laboratory of Disaster Reduction in Civil Engineering, Tongji University, Shanghai 200092, China
[b] Dept. of Structural Engineering, Tongji University, Shanghai 200092, China

ARTICLE INFO

Keywords:
Acoustic emission
Wavelet transform
Time-frequency diagram
Deep learning
Slip-critical blind bolt
Bolted connection monitoring

ABSTRACT

Bolt preload is a crucial factor in high-strength bolt applications, particularly for the Slip-critical blind bolts (SCBBs). This study presents a novel nondestructive approach that leverages ultrasonic echo waves to accurately detect the state of bolt looseness, addressing a significant research gap in the field of blind bolt looseness detection. The proposed technique is uniquely suitable for blind bolted connections as it only necessitates access to a single side of the connection. Nine types of SCBBs were tested and obtained approximately 4000 ultrasonic echo signals with varying degrees of looseness. These signals have been transformed into image-based representations using wavelet analysis, and deep learning techniques were used to classify and predict the looseness level accurately. The performance of various damage assessment criteria, CNN models, and dataset sizes were evaluated and compared. The proposed method was validated by classifying 400 datasets with a validated accuracy of 97.30%.

1. Introduction

Preload is crucial for the mechanical performance of high-strength bolts, particularly the slip-critical type, as it enhances the connection's reliability and affects its overall performance [1–3]. It has been proved that the loss of the preload in the high strength bolt group will reduce the connection strength and stiffness dramatically [4]. Various techniques have been developed to measure bolt pretension in situ, such as [5–7], piezoelectric active sensing method [8,9], acoustoelastic effect-based method [10] and so on [11]. However, the challenge of monitoring the looseness level of bolt preload with higher precision and cost-effectiveness to facilitate the application in practice remains enormous. On the other hand, the slip-critical blind bolt (SCBB) poses a greater challenge for monitoring preload due to its special design for connecting hollow section columns (HSC) and achieving high preload with only one-side access [12,13]. As a result, few techniques are applicable to this scenario. One such method is vision-based methods, which have gained popularity recently [11]. It relies on the loosening angle as the monitoring objective. Unfortunately, when a bolt shank loses 30% of its preload, it only results in less than 0.5 degrees of nut rotation [14]. Therefore, accurately defining the rotation angle close to 0 degrees using vision-based methods becomes challenging. Another method to address the above challenge is the acoustoelastic effect-based technique, utilizing acoustic emission (AE) signals. It has many advantages such as low cost and rapid construction speed [10,15–19]. It also has a short coming that a relatively cumbersome calibration process is required to obtain individual calibration constants for each type of bolt during previous experimental verifications.

Meanwhile, AE signals has been applied for detecting and locating damage in numerous structural components, including beams, slabs, walls, and full-scale structures [20], while the use of AE signals in the monitoring of bolts still is a rarefied [21]. Zhang et al. [22] installed AE sensors on connecting plates and used intrinsic mode functions of AE signals to monitor the tightening condition of single-lap bolted joints. But the method still has no ability to monitor the multi-type of joint with some other surface properties. It's worth furthering the use of AE signals, but better in other ways to expand the scope of applicability.

Most of the deep learning-based methods have been used for the identification of the looseness of bolts by recognizing the change of the configurations visually, which are bad at capturing the precise change of preload directly as mentioned above. Some of these methods utilize sound signals [23], percussion-induced signals [24,25] or impedance-based signals [26], hinting the possibility of applying the deep learning to obtain the damage information in wave signals. There

* Corresponding author at: State Key Laboratory of Disaster Reduction in Civil Engineering, Tongji University, Shanghai 200092, China.
E-mail address: weiwang@tongji.edu.cn (W. Wang).

https://doi.org/10.1016/j.istruc.2024.106521
Received 13 December 2023; Received in revised form 15 April 2024; Accepted 30 April 2024

also exists some studies using deep learning to analyze the AE signals, with the intention of damage detection and fault diagnosis. Madhusudana et al. [27] presented a novel fault diagnosis approach utilizing a decision tree and acoustic signal wavelet transform. This technique can effectively detect and monitor the surface roughness, dimensional tolerances, and tool status of the milling cutter. The integration of AE signals has shown promising results in detecting and localizing damages in various one-dimensional and two-dimensional structural members, including wooden and concrete beams [20]. It has also been applied to rail crack monitoring, with synchrosqueezed wavelet transform to process the AE data [28]. But this method with the combination of the AE signals and deep learning for bolt preload monitoring is still a relatively unexplored area of research. A common benchmark was created for comparing data-driven methods in such cases [29].

They introduced a method for identifying multi-bolt loosening through vibro-acoustic modulation signals. However, this approach was exclusively validated for a specific connection involving four bolts. It didn't establish a universal correlation between monitoring outcomes and the general loss of bolt pretension, which severely limited the applying range of the method. Zhang and Liu [30] recognized the state of flange bolt connection by extracting the eigenvalues of Mel-frequency cepstral coefficients of AE signals and then using deep learning to identify the features. Emmanuel Ramasso et al. [21] built a dataset made of raw AE data streams and used supervised and unsupervised deep learning to monitor loosening in two bolted plates. However, none of them is targeting blind bolts.

In this paper, a method based on AE signals, referring to ultrasonic echoes is developed to detect the preload looseness in SCBB, which has the tor-shear bolt shank. This study has carried out a series of experiments with different configurations of SCBBs. After achieving thousands of ultrasonic echo waves during the experimental process, wavelet analysis provides an efficient way to transform the signals into image information. And deep learning can classify the image and predict the preload level in SCBB. The workflow of the proposed method, including the process of dataset construction, suitable for real construction sites is given. The performance of different damage assessment criteria, different convolutional neural network (CNN) models and different dataset sizes are compared and assessed as well. After choosing the best criterion, CNN model and dataset size, the proposed method is validated by classifying 400 data precisely and effectively. Diverging from many deep learning-based approaches for visual recognition, this methodology harnesses the inherent strengths of deep learning while not focusing on identifying objects based on the connections' appearance, which has been approved to be invalid. It provides a good choice for detecting the damaged bolted connections on practical projects, especially for blind bolted connections.

2. Methodology

The primary objective of this approach is to differentiate the damage data from the AE signals for SCBB connections. The proposed approach's workflow is depicted in Fig. 1. In the first step, the raw time series dataset collected from the laboratory is transformed into image information in the form of scalograms using continuous wavelet transform (CWT). The primary goal of visualizing the time series dataset is to utilize deep learning on the dataset to extract the damage data eventually. In the subsequent step, a CNN model is trained using the dataset obtained in the preceding step. By utilizing the well-trained CNN model, the various types of bolt preload looseness can be identified for the detection data acquired on site. Then the condition of the bolts can then

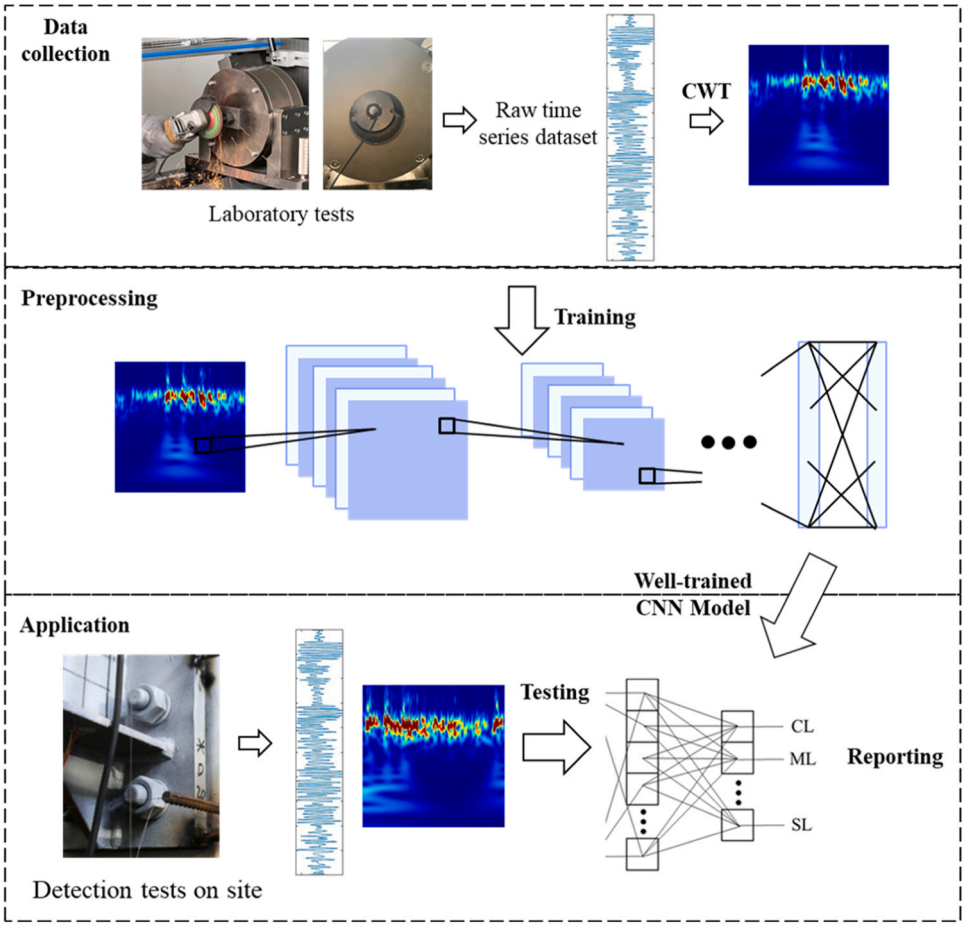

Fig. 1. Workflow of the proposed method.

be reported and analyzed.

2.1. Wavelet analysis

Wavelet analysis is a mathematical method for decomposing a signal into different frequency components, which can provide time and frequency information about the signal. It has the characteristics of multi-resolution analysis and has the ability to represent local features of signals in both time and frequency domains. It is a time-frequency localization analysis method with a fixed window size but a changeable shape, where both the time window and the frequency window can be changed. That is, it has a lower time resolution and a higher frequency resolution in the low-frequency part, and a higher time resolution and a lower frequency resolution in the high-frequency part, suitable for analyzing non-stationary signals and extracting local features of signals [31,32].

The CWT is the widely used and efficient wavelet analysis tool for analyzing signals in the time- frequency domain. It provides a continuous, scale-varying representation of a signal, allowing for the analysis of both the frequency content and the localization of the frequency content over time. CWT is ideal for analyzing non-stationary signals and can provide a more detailed time-frequency representation. It is computed by convolving the signal $x(t)$ with a wavelet function that is translated and scaled in time:

$$W_{u,s} = \int_{-\infty}^{\infty} x(t)\varphi^*_{u,s}(t)dt \tag{1}$$

$$\varphi^*_{u,s}(t) = \frac{1}{\sqrt{s}} e^{j\omega_0\left(\frac{t-u}{s}\right)} e^{-\frac{(t-u)^2}{2s^2}} \tag{2}$$

where $\varphi^*_{u,s}(t)$ represents the complex conjugate of the wavelet basis function, which is called the mother wavelet or Complex Morlet wavelet. ω_0 is the center frequency of the wavelet function. The scale variable s and the transitional variable u in the wavelet transform represent the width and location of the wavelet window, respectively. Specifically, the scale s determines the frequency band of the wavelet function, while the translation u defines the position of the moving window. The MATLAB wavelet toolbox is employed in this study to use the functions.

2.2. Convolutional Neural Network (CNN)

The CNN is a type of artificial neural network that is used in computer vision and image recognition tasks. It is designed to process grid-structured data, such as an image, by performing convolution operations on the input image to learn and extract meaningful features from the data. The basic building block of a CNN is a convolutional layer, where a small matrix called a filter is convolved with the input data to produce a feature map. The filter slides over the input data, element-wise multiplying and summing the overlapping elements to produce a new feature map. This process allows the network to learn spatial hierarchies of features, where lower-level features are combined to form higher-level features, that can capture the most relevant information from the input data. After several convolutional layers, the feature maps are passed through a pooling layer, where the spatial resolution of the data is reduced to reduce the computational cost of the network and improve the robustness of the features. A common pooling method is max pooling, where the maximum value in each pooling region is taken to produce the new feature map. Finally, the feature maps are flattened and passed through a fully connected layer, where each neuron in the layer is connected to all neurons in the previous layer. The fully connected layer outputs the prediction of the network, which is usually followed by a loss function, such as cross-entropy, that measures the difference between the network prediction and the ground truth. The gradients of the loss function with respect to the network parameters are then computed and used to update the network parameters in a process called backpropagation.

One of the advantages of CNNs is that they can learn to recognize patterns in images that are invariant to translation, scaling, and other geometric transformations. This is achieved by using convolution and pooling layers that have shared parameters, meaning that the same weights are used for multiple locations in the input data. This allows the network to learn translations and other geometric transformations of the same pattern, making it robust to small variations in the input data.

Convolutional Neural Networks are powerful tools in the field of computer vision and image recognition. By using convolution, pooling, and fully connected layers, CNNs can learn meaningful features from the input data and produce accurate predictions for a wide range of image classification tasks.

Among many CNN models, ResNet-50 CNN model has been proved to have high efficiency and good performance [33], even in the field of bolt loosening identification [29]. ResNet introduced the concept of residual connections between its layers, which greatly improves the training process by reducing the loss, maintaining knowledge gain, and enhancing performance. In a residual connection, the output of a layer is simply the sum of its input and a convolution of that same input..

3. Experimental Verification

3.1. Specimens and Test Setup

Nine groups of specimens are tested in this study. The bolt size varies from 16 to 24 mm and the range of grip length is from 30 to 100 mm, which is aimed to extend the size and multiplicity of dataset and improve the generalization ability of the CNN model. The configurations of specimens are listed in Table 1. All the bolts are tor-shear type [34]. Here “Number” means the number of specimens having the same configuration in each group. The bolt loads transition from zero to the values indicated as load range in Table 1. The load range is determined by the bolt itself, as the torque-shear type bolt reaches its final pretension when the tail end is twisted off. Each specimen was labeled as *M*D-*L*-*n*, where *D* is the bolt diameter in millimeters, *L* is the grip length, *n* denotes the specimen number in the same group. All the signal data in this study is generated from these 36 specimens, considering different bolt diameters, grip length and bolt length.

The test set-up, as depicted in Fig. 3, comprises essential components such as the bolt load controlling system, data acquisition system, and so on. In this setup, piezoelectric (PZT) sensors serve the dual purpose of generating ultrasonic waves and capturing echo signals. Notably, a ring-shaped pressure sensor with a 20 t range is employed here to achieve precise pretension in bolts, as illustrated in Fig. 3. A temperature sensor was supposed to measure the change of the temperature. However, due to the limit of experimental condition, the influence of temperature is not considered here. The change of room temperature was around 6 C, which didn’t have significant impact on the measured results for time-of-flight (TOF) method [34]. The bolt load controlling system applies torque to the bolts, enabling force adjustments with a loading rate of approximately 10 kN/min. This experimental configuration has previously been employed in a study involving an ultrasonic technique [34], albeit with data collection focusing on TOF rather than the echo signals analyzed in the current investigation.

The process of collecting ultrasonic echo waves is shown in Fig. 4. For each measurement, only one PZT patch needs to be installed. The probe, for generating and receiving the signals, can be used for all types of specimens. The manufacturer of the equipment and probe is Shanghai Tiancheng Industrial Co. Ltd., China. When the detection tests need to be conducted on site, i.e. at the third step of the workflow in Fig. 1, the signal generator and data acquisition system is the only instrument that is necessary. It is the portable suitcase in Fig.3(b), which makes the technique more possible to be applied on real sites.

Unlike the previous studies which were based on the ultrasonic technique, this method doesn’t consider the influence of bolt size and

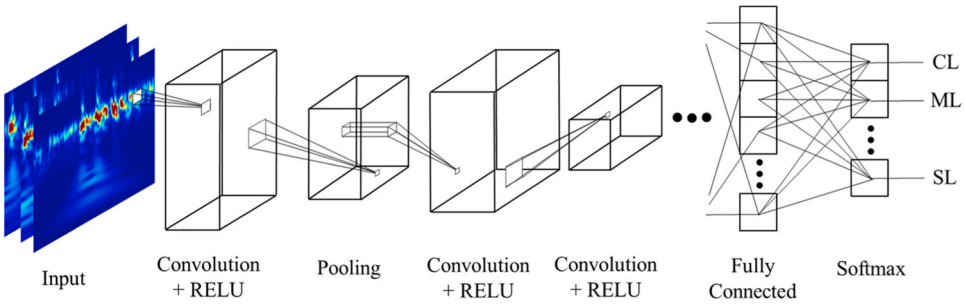

Fig. 2. Framework of a CNN model used in this method.

Table 1
Configurations of specimens.

Specimen No.	Bolt diameter (mm)	Grip length (mm)	Total length (mm)	Number	Load range (kN)
M16-40	16	40	80	4	99.6
M20-40	20	40	80	4	191.3
M24-30	24	30	70	4	264.0
M24-40		40	80	4	259.4
M24-50		50	90	5	228.9
M24-51		51	100	4	200.2
M24-60		60	100	3	272.0
M24-80		80	120	4	262.3
M24-100		100	140	4	258.1

clamping length. The dataset would be built by integrating the data of all specimens. The first task is to define the damage criterion and give the labels to each data. Then transform the wave data to images that can be identified by CNN models.

3.2. Damage assessment criteria and time-frequency diagram

The first criterion is based on the individual bolt. The baseline is the initial pretension load in the bolt shank when the tail is just twisted off. In this study, a standard preload of 225 kN is established for M24 bolts, while the subsequent sizes, M20 and M16 bolts, should maintain a preload of 155 kN and 100 kN respectively. This indicates that if the M24 bolt loses approximately 30% of its preload, it would function equivalently to a smaller M20 bolt. Furthermore, a 60% reduction would restrict its functionality to that of the smallest M16 bolt. Likewise, for an M20 bolt, a 30% reduction in pretension would result in it operating solely as an M16 bolt. Hence, a 30% loss in preload has been selected as the threshold for determining this step. To be specific, if the preload loss in the bolt is less than 30%, the damage state would be defined as slightly loosening (SL); if it's between 30% and 60%, the damage would be assessed as moderate loosening (ML); if the loss is larger than 60%, the damage state would be critical loosening (CL). According to the first criterion, three random ultrasonic echoes of different damage categories are chosen from the data obtained during the tests, whose signal diagrams are shown in Fig. 5. Interpreting the state of the bolt directly from their individual signal shapes proves to be impractical in real-time on-site scenarios. Automating this process becomes crucial, and this study achieves it through the implementation of a deep learning method, providing an efficient and automatic means of reading the bolt's state.

The second criterion is based on the stress level at the clamping area. When the pretension in tightened bolt satisfies the specification [35,36], the tensile stress in the clamping area of the bolt shank should be around 635 MPa. If the stress value is larger than 445 MPa, the damage state

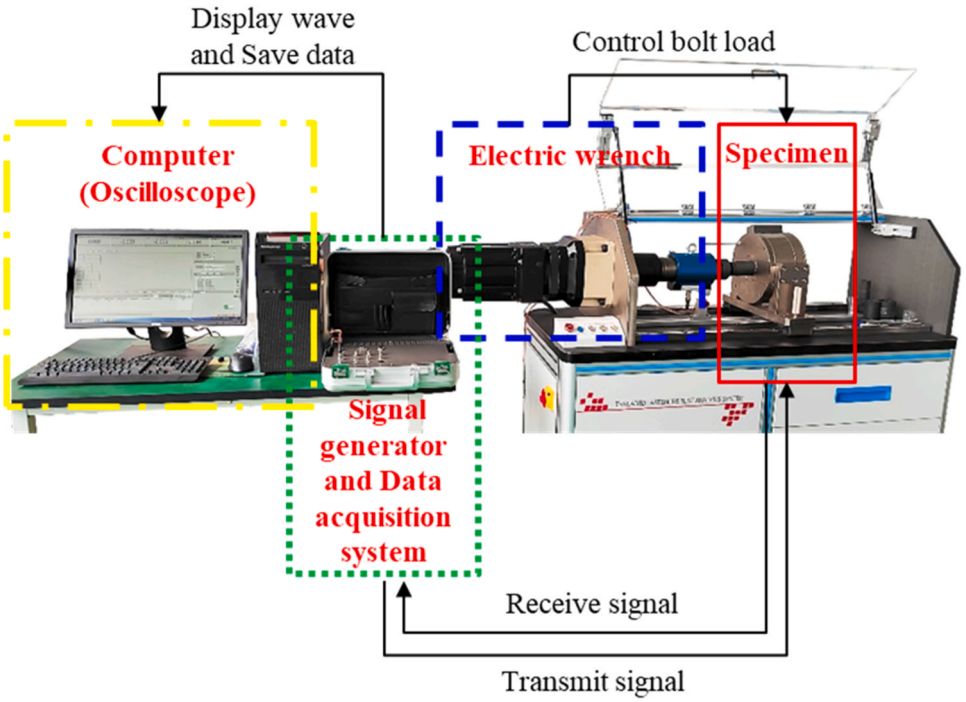

Fig. 3. Test set-up [34].

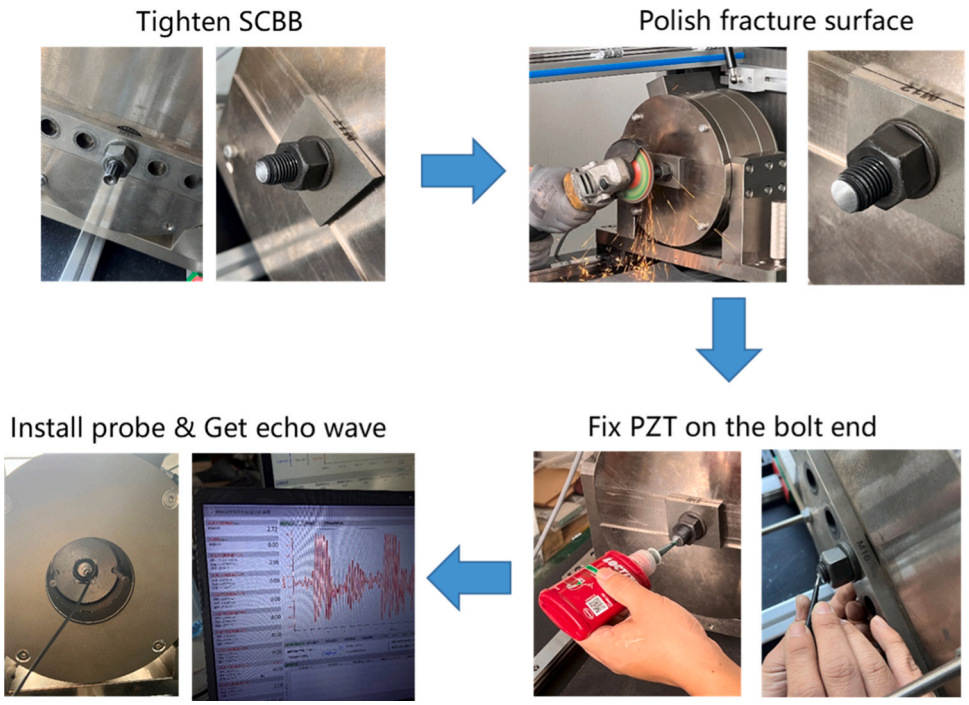

Fig. 4. Process of collecting the signals.

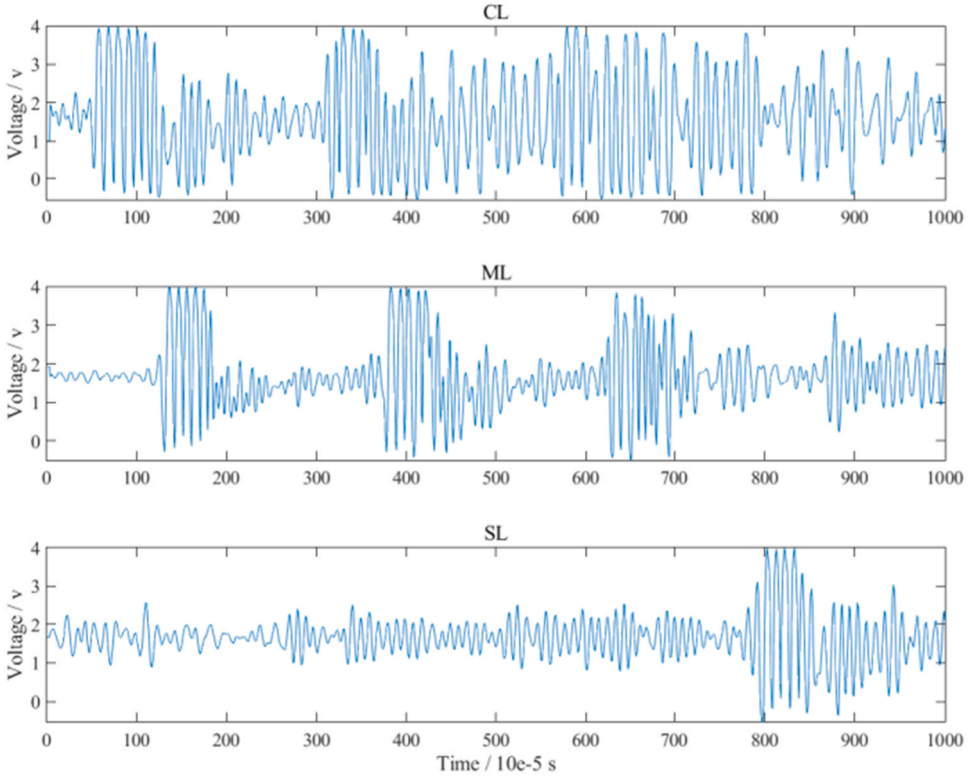

Fig. 5. Ultrasonic echoes at the first 0.01 s for each kind of damage categories.

would be defined as slightly loosening (SL); if it is in the range of 225–445 MPa, the damage would be assessed as moderate loosening (ML); if the tensile stress in the bolt shank is less than 255 MPa, the damage state would be critical loosening (CL). The stress is achieved by dividing the measured pretension load by the cross-sectional area of the bolt shank.

Based on different damage assessment methods, distinct labels have been defined, resulting in the creation of two final datasets. The construction of datasets will be discussed in the next section. These datasets exhibit minimal differences, comprising the same signals, with only a few instances possessing varying labels. The reason is the bolt shanks were fabricated according to the strict requirements of the Chinese

standard [35], which means their initial stress levels would be within a certain range. But these distinctions still result in different performances during the analysis, which will be described in Section 4.

The first criterion based on the bolt load was proposed because the bolt load was the primary subject that this research focused on. The bolt load has always been one of the most important design parameters for high strength bolts in the standards or codes. But in this criterion, the baseline is the initial pretension that the bolt achieves at the very beginning. It means that the initial pretension needs to be measured and the labels should be decided individually for each bolt. Then the second criterion was proposed to get a common definition of labels for all the bolts.

3.3. Dataset construction

The construction of datasets will be introduced in detail here. As mentioned in Section 2, the main idea of this method is to collect the ultrasonic echo waves labeled with damage levels and then train the CNN model to learn how to distinguish the damage information in the wave data. During the tests, a total of 3964 echo waves have been achieved and tagged with various pretensions. They are all from the specimens described in Section 3.1.

To consider the frequency features in the ultrasonic wave data and the temporal evolution, a CWT analysis is carried out on the relevant data. CWT is applied to produce the time-frequency representation of the ultrasonic echoes with around 2000 data points, which are the whole segments of signals achieved in the experiments. The output of the CWT is a 2D array, where the rows correspond to different scales (or frequencies) and the columns correspond to different time points. Each element of the array represents the strength or energy of the wavelet coefficient at that particular scale and time. To visualize the results better, the CWT coefficients are squared to obtain the power or energy at

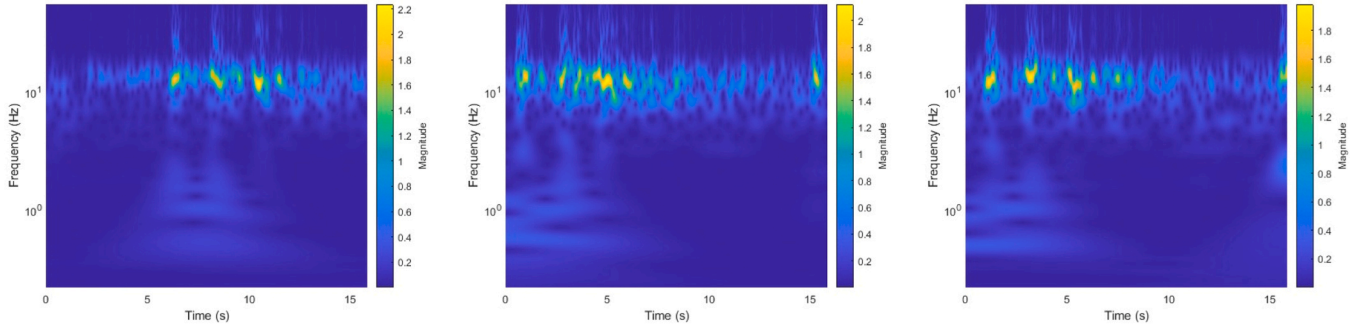

(a) Slightly loosening (SL)

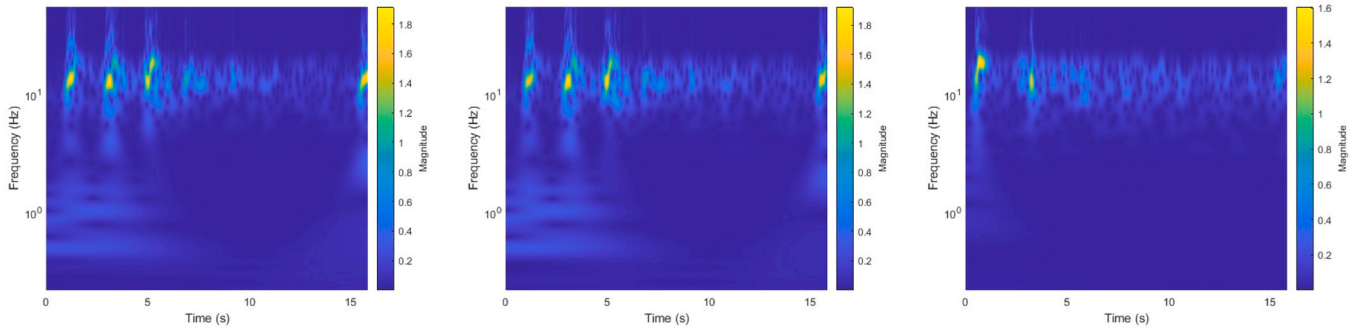

(b) Moderate loosening (ML)

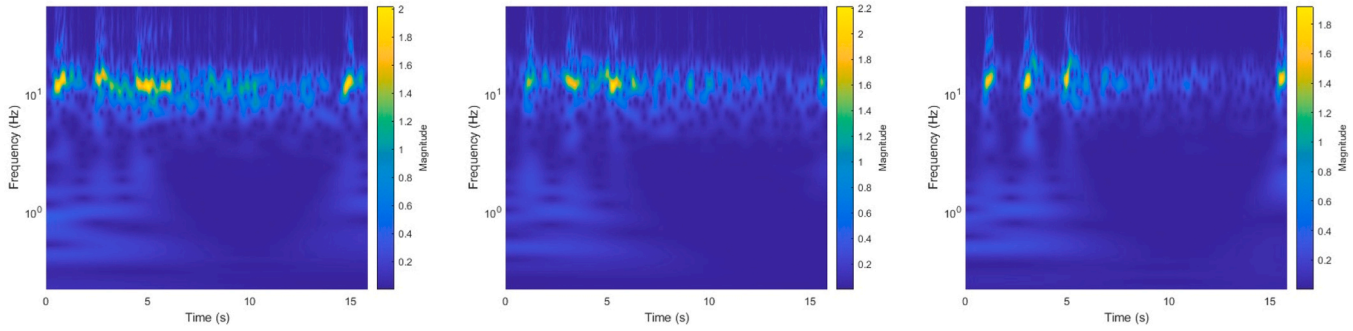

(c) Critical loosening (CL)

Fig. 6. CWT spectrograms under different damage conditions.

each scale and time, and the resulting 2D array is plotted as a heatmap, referred to as scalograms, as illustrated in Fig. 6. The frequency scale is represented on the y-axis, while the time scale is represented on the x-axis. At the same time, the scalograms are saved as RGB figures with sizes of 224 × 224×3 or 227 × 227×3 (depending on the inputting requirement of CNN models). In the analytical process, the data set will be randomly split into two groups in each analysis. The first group, consisting of 80% of the original data set, will be utilized for training. The remaining 20% will be reserved for validation purposes.

3.4. Training of the networks

The choice of hyperparameters is critical to deep learning [37]. Most of the hyperparameters have been decided by following the instructions from previous studies [29,37]. The training batch (Minibatch) size is 15, and the round (MaxEpoch) is 20. The initial learning rate is 1e-4. The monitoring index is the average absolute error. The damage function is the mean square error. A dropout layer with a probability of 0.6 is set to randomly drop 60% of nodes, with the aim of avoiding overfitting further. Other initial parameter weights are given by MATLAB, which are pretrained on the ImageNet dataset. The CNN program has been written and run with MATLAB R2022a. The details of the computer platform and environment configuration are shown in Table 2.

4. Results and discussion

4.1. Comparison of different damage assessment criteria

As mentioned in Section 3.2, this research has proposed two different damage assessment criteria.

166 samples are adopted here to compare the performance of two kinds of damage assessment criteria. The comparison results are summarized in Table 3. Both criteria have 100% accuracy in the training dataset, while the second one has much higher accuracy in the validation dataset, as 97.0%. It also means the second criterion would have a smaller probability of error in prediction if it's applied on real sites. And the final training loss of that criterion is only 0.0008 and the validation loss value is 0.1545. Overall, the second criterion has better performance.

Besides, the criterion based on the stress-level value of the bolt shank could compare all the SCBBs on the same level and get the health condition of SCBBs directly. It also makes the process of dataset construction easier by giving the labels (preload loss level) without a demand for knowing the initial pretension in the bolt shanks. Hence the second criterion would be chosen in this method, which is also used in the following analysis.

4.2. Comparison of different CNN models

To choose the most effective and adaptive CNN model for this research, six classical models are compared here in total, including GoogLeNet, SqueezeNet, AlexNet, VGG-19, ResNet-50, and MobileNetv2. The complete dataset created in Section 3.3 is utilized for this part. The training parameters are uniformly established throughout the training and validation process to ensure optimal comparability, which also follows the description in Section 3.4. Fig. 7 depicts the accuracy and loss rate curves of all the models using the training or validation datasets. The summarized results of accuracy and loss are presented and compared in Table 4.

Table 2
Computer platform and environment configuration.

Software and hardware platform	Model parameters
Operating system	Windows 11 a 64-bit system
CPU	Intel(R) Core (TM) i7-7700
GPU	AMD Radeon R7 450
Memory	16 GB
Programmed environment	MATLAB R2022a

Table 3
Comparison of performance with different damage assessment criteria.

Criterion	Accuracy (%)[38]		Loss[38]	
	Training Dataset	Validation Dataset	Training Dataset	Validation Dataset
First	100.0	91.2	0.0009	0.2223
Second	100.0	97.0	0.0008	0.1545

As shown in Fig. 7, all the models converge at about 1500 iterations. Though the training curves of the models except ResNet-50 still have fluctuation after that, the validating curves stay smooth at the later stage. Out of all the models, ResNet-50 exhibits the quickest convergence and attains the highest validation dataset accuracy. It converges after only 200 iterations. Additionally, it has the lowest loss values for both the training and validation datasets, which are 0.0002 and 0.0515 respectively. AlexNet model has the opposite performance with the lowest accuracy for the validation dataset and high loss value for both the training and validation datasets. SqueezeNet and GoogLeNet have poor performance of convergence as well, which is clearly shown in Fig. 7(b). VGG-19 had the largest loss value for the validation dataset. MobileNetv2 demonstrates favorable convergence speed and low loss values compared to the other models, excluding ResNet-50. However, its accuracy in predicting damage situations on the validation dataset is below 97%. Taken together, ResNet-50 exhibits the most superior performance and, as such, has been selected as the optimal CNN model employed in this study. Subsequent analyses will accordingly adopt this model.

4.3. Sensitivity analysis of dataset size

The extraction of nonlinear features is dependent on images, which are sourced from various datasets. The recognition performance of the model is largely determined by the dataset used. To investigate the impact of dataset size on the outcomes, and also to decide the most suitable dataset size for the proposed method, eleven different dataset sizes ranging from 200 to 3964 are chosen for model training. The new datasets are formed by randomly selecting data from the original dataset. ResNet-50 model, which is mentioned and compared in the last section, is adopted here. Table 5 shows the accuracy of models trained using five different dataset sizes.

It is evident that the accuracy of the model on the validation dataset increases as the dataset size grows, particularly when the dataset size is less than 2000. The training dataset consistently achieves a perfect accuracy score of 100%. Across the various dataset sizes, the validation accuracy ranges from 91% to 98.4%. Impressively, even with only 1000 images in the dataset, the ResNet-50 model still achieves a high accuracy rate of 95% on the test dataset.

To ensure that the model has a higher accuracy and generalization capability, it is crucial to have sufficient image samples. This ensures that the model can learn subtle nonlinear features and differentiate between similar features [27]. The variation in verification accuracy and test accuracy is minimal when the dataset size exceeds 2000. Table 5 shows that with a dataset size of 2000, the validation accuracy is 98.3%, and the loss values for the training and validation datasets are only 0.0003 and 0.0566, respectively. In summary, with a dataset size of 2000, the ResNet-50 model achieves remarkable recognition performance, with stable and strong generalization ability.

4.4. Validation of the proposed method

This part is intended to validate the proposed method with the recommended criterion, CNN model and dataset size. A ResNet-50 model

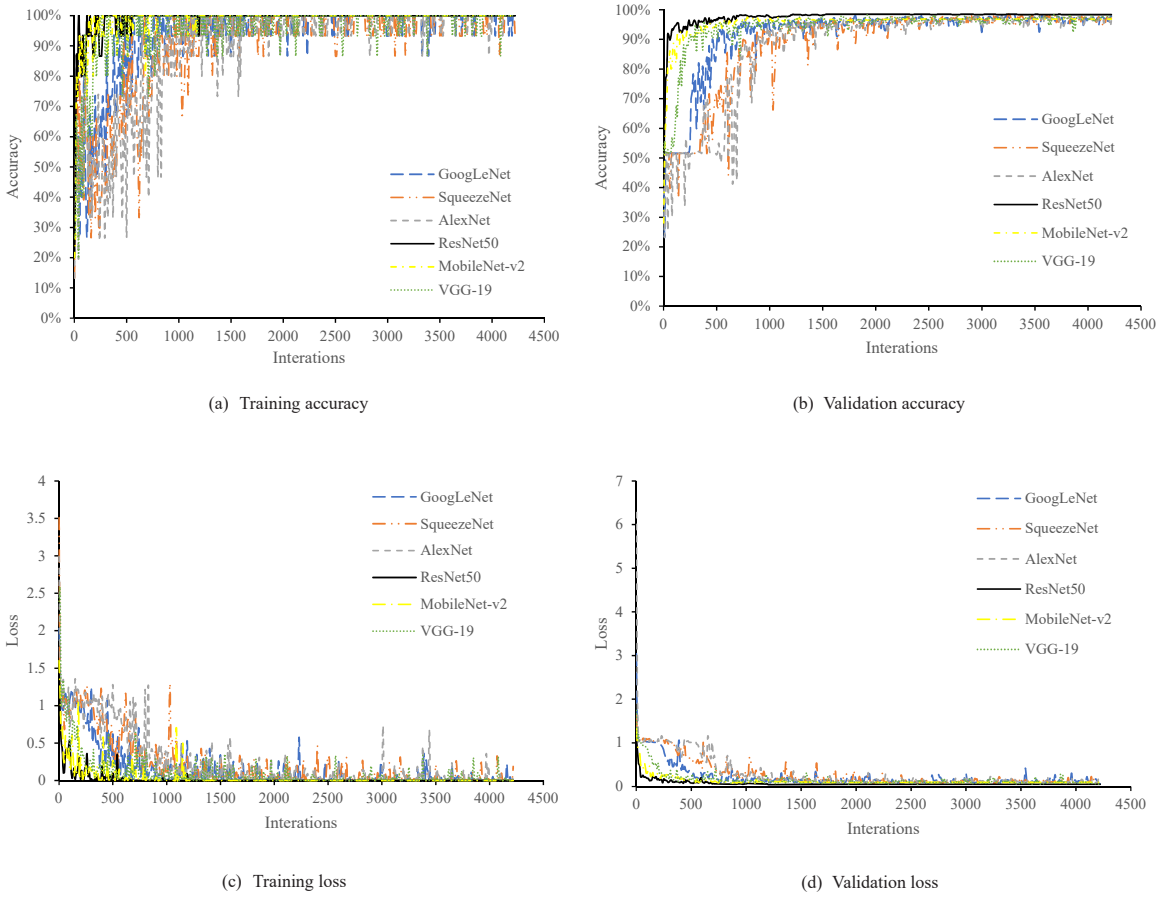

(a) Training accuracy (b) Validation accuracy

(c) Training loss (d) Validation loss

Fig. 7. Comparison of different CNN models.

Table 4
Comparison of performance of different CNN models.

CNN model	Accuracy (%)		Loss	
	Training Dataset	Validation Dataset	Training Dataset	Validation Dataset
GoogLeNet	100.0	97.9	0.0029	0.0607
SqueezeNet	100.0	97.2	0.0008	0.0808
AlexNet	100.0	96.2	0.0021	0.1203
ResNet-50	100.0	98.4	0.0002	0.0515
MobileNetv2	100.0	96.9	0.0004	0.0962
VGG-19	100.0	97.0	0.0008	0.1545

Table 5
Comparison of performance of different dataset size.

Dataset size	Accuracy (%)		Loss	
	Training Dataset	Validation Dataset	Training Dataset	Validation Dataset
200	100.0	92.5	0.0008	0.3333
500	100.0	91.0	0.0005	0.3273
1000	100.0	95.0	0.0002	0.1529
1500	100.0	94.7	0.0001	0.1663
1800	100.0	97.5	0.0001	0.0674
1900	100.0	98.2	0.0002	0.0428
2000	100.0	98.3	0.0003	0.0566
2500	100.0	97.6	0.0002	0.0889
3000	100.0	98.0	0.0003	0.0475
3500	100.0	98.1	0.00001	0.1116
3964	100.0	98.4	0.0002	0.0515

trained by the above 2000 dataset based on the second criterion is used here to judge the damage levels of some new data. The confusion matrix and some classification indexes, e.g. Precision, Recall, False positive rate and F1-score [25,29], are applied here to assess the performance of the proposed method, as shown in Fig. 8 and Table 6. The Precision, Recall, False positive rate and F1-score can be calculated as following equations.

$$\text{Precision} = \frac{TP}{TP + FP} \tag{3}$$

Fig. 8. Confusion matrix.

Table 6
Classification performance of the proposed method.

Label	Precision (%)	Recall (%)	False positive rate (%)	Fl-score
CL	99.02	98.06	0.01	0.99
ML	96.74	95.70	0.01	0.96
SL	96.15	99.01	0.01	0.98
Average	97.30	97.59	0.01	0.98

$$\text{Recall} = \frac{TP}{TP + FN} \tag{4}$$

$$\text{Falsepositiverate} = \frac{FP}{TN + FP} \tag{5}$$

$$\text{Fl} - \text{score} = \frac{2 \times \text{Precision} \times \text{Recall}}{\text{Precision} + \text{Recall}} \tag{6}$$

where TP is True Positive, i.e. true class and predicted class are both positive. FP is False Positive, i.e. true class is negative, while predicted class is positive. TN is True Negative, i.e. true class and predicted class are both negative. FN is False Negative, i.e. true class is positive, while the predicted class is negative [25].

On average, the precision across all three labels indicates that the trained ResNet-50 model has an overall accuracy of 97.30%. Furthermore, the model exhibits exceptional performance on the CL class, with a precision exceeding 99% and an F1-score surpassing 0.99. Notably, the false positive rates for all classes are as low as 0.01. These results affirm that the proposed method, with its unique criterion, CNN model, and dataset size, is proficient in detecting damage information from ultrasonic echoes and accurately classifying damage levels.

5. Concluding remarks

Bolt preload plays a key role in ensuring the stability and structural integrity of bolted connections, as improper or inadequate preload can lead to premature failure or reduced performance of the system. However, monitoring bolt preload accurately and reliably has proven to be a formidable challenge, particularly in the case of high-strength SCBB preload loosening. This challenge arises due to the difficulty in assessing bolt preload non-destructively and one-side, as conventional inspection methods such as visual examination or torque measurement may not provide adequate or accurate information on the actual preload level. In this paper, a damage detection technique for identifying bolt load looseness, especially for SCBBs equipped with tor-shear bolt shanks is presented. This innovative approach leverages the utilization of AE signals, wavelet analysis, and deep learning techniques, to deliver a comprehensive and precise damage detection system.

Nine kinds of SCBBs have been tested in this research. About 4000 ultrasonic echo signals have been gotten with various degrees of looseness. And the dataset has been built based on these signals. Wavelet analysis offers a powerful and efficient means of transforming signals into image-based representations, while deep learning techniques can effectively classify these images and accurately predict the looseness level in SCBB. This paper also encompasses a comprehensive workflow and a practical dataset construction process specifically designed for deployment on real construction sites. The performance of various damage assessment criteria, CNN models, and dataset sizes are thoroughly evaluated and compared. Notably, the criterion based on the stress-level value of the bolt shank demonstrates superior performance, while the ResNet-50 CNN model achieves the best generalization ability and the most accurate nonlinear feature extraction among all the CNN models evaluated. Moreover, a dataset size of 2000 is deemed the most effective and reasonable. Following the identification of the optimal combination of factors, the proposed method is validated by accurately and effectively classifying 400 datasets, achieving a validated accuracy of 97.30%.

This method has overcome the shortness of the detecting technology based on TOF, which needs individual calibrations for each kind of bolt. In addition, compared with other methods like the popular vision-based method, the proposed technique boasts exceptional identification accuracy and stability, ensuring reliable and consistent detection of bolt looseness. The detecting device itself is also highly portable and compact, enabling easy deployment and integration into real-world applications with minimal disruption. This feature enhances the applicability and versatility of the technique, making it well-suited for a wide range of industrial and structural settings. With these advanced capabilities, the proposed technique represents a significant advancement in the field of bolted connection monitoring, especially blind bolted connection monitoring and has the potential to transform the way in which bolt preload is assessed and managed, particularly in safety-critical applications where reliability and performance are of utmost importance. This technique hasn't had the opportunity to be applied on site. Future work will be conducted out of the laboratory to discuss the influence of complex environmental situations.

CRediT authorship contribution statement

Xing Gao: Conceptualization, Data curation, Formal analysis, Investigation, Methodology, Software, Validation, Visualization, Writing – original draft, Writing – review & editing. **Wei Wang:** Funding acquisition, Project administration, Resources, Supervision, Writing – review & editing. **Jiajun Du:** Conceptualization, Supervision, Writing – original draft, Writing – review & editing.

Declaration of Competing Interest

The authors declare that they have no known competing financial interests or personal relationships that could have appeared to influence the work reported in this paper.

Acknowledgments

The financial supports from the Natural Science Foundation of China (NSFC) with Grant Nos. 52378182, 52078366 and National Key Research and Development Program of 14th Five-Year Plan of China with Grant No. 2022YFC3801900 are gratefully acknowledged. This study is also supported by the Top Discipline Plan of Shanghai Universities-Class I with Grant No. 2022–3-YB-18 and Shanghai 2022 Science and Technology Innovation Action Plan Social Development Science and Technology Research Project with Grant No. 22dz1201700.

References

[1] Yu Q, Zhou H, Wang L. Finite element analysis of relationship between tightening torque and initial load of bolted connections. 1687814015588477 Adv Mech Eng 2015;7. https://doi.org/10.1177/1687814015588477.
[2] Oktavianus Y, Goldsworthy HM, Gad E. Group behavior of double-headed anchored blind bolts within concrete-filled circular hollow sections under cyclic loading. J Struct Eng 2017;143:04017140. https://doi.org/10.1061/(ASCE)ST.1943-541X.0001882.
[3] Cabrera M, Tizani W, Ninic J, Wang F. Experimental and numerical analysis of preload in Extended Hollo-Bolt blind bolts. J Constr Steel Res 2021;186:106885. https://doi.org/10.1016/j.jcsr.2021.106885.
[4] Kong Q, Li Y, Wang S, Yuan C, Sang X. The influence of high-strength bolt preload loss on structural mechanical properties. Eng Struct 2022;271:114955. https://doi.org/10.1016/j.engstruct.2022.114955.
[5] Cha Y-J, You K, Choi W. Vision-based detection of loosened bolts using the Hough transform and support vector machines. Autom Constr 2016;8.
[6] Ramana L, Choi W, Cha Y-J. Fully automated vision-based loosened bolt detection using the Viola–Jones algorithm. Struct Health Monit 2018;13.
[7] Ramana L., Choi W., Cha Y.-J. Automated Vision-Based Loosened Bolt Detection Using the Cascade Detector. In: Sit E.W., Walber C., Walter P., Seidlitz S., editors. Sens. Instrum. Vol 5, 2017, p. 23–28. https://doi.org/10.1007/978–3-319–54987-3_4.
[8] Wang F, Huo L, Song G. A piezoelectric active sensing method for quantitative monitoring of bolt loosening using energy dissipation caused by tangential damping based on the fractal contact theory. Smart Mater Struct 2018;27:015023. https://doi.org/10.1088/1361-665X/aa9a65.

[9] Huo L, Wang F, Li H, Song G. A fractal contact theory based model for bolted connection looseness monitoring using piezoceramic transducers. Smart Mater Struct 2017;26:104010. https://doi.org/10.1088/1361-665X/aa6e93.
[10] Rose JL. Ultrasonic Guided Waves in Solid Media. New York: Cambridge University Press; 2014. https://doi.org/10.1017/CBO9781107273610.
[11] Huang J, Liu J, Gong H, Deng X. A comprehensive review of loosening detection methods for threaded fasteners. Mech Syst Signal Process 2022;168:108652. https://doi.org/10.1016/j.ymssp.2021.108652.
[12] Gao X, Wang W, Teh LH. A novel slip-critical blind bolt: experimental studies on shear, tensile and combined tensile-shear resistances. Thin-Walled Struct 2021; 170:108630. https://doi.org/10.1016/j.tws.2021.108630.
[13] Wang W, Chen Y, Jian X. Cyclic behavior of endplate connections to tubular columns with novel slip-critical blind bolts. Eng Struct 2017;148:949–62. https://doi.org/10.1016/j.engstruct.2017.07.015.
[14] Jiang Y, Zhang M, Lee C-H. A study of early stage self-loosening of bolted joints. J Mech Des 2003;9.
[15] Han Y, Wu F, Li M, Mei J, Wang X. Factors influencing measurement of bolt stress based on acoustoelastic effect (in Chinese). J Cent South Univ Sci Technol 2020;51: 359–66.
[16] Jia X, Wang X, Gan W, Ni W. Research on calibration of bolt's axial stress based on acoustoelastic effect (in Chinese). China Meas. Test 2018;44:23–7.
[17] Chaki S, Corneloup G, Lillamand I, Walaszek H. Combination of longitudinal and transverse ultrasonic waves for in situ control of the tightening of bolts. J Press Vessel Technol-Trans ASME 2007;129:383–90. https://doi.org/10.1115/1.2748821.
[18] Ding X, Wu X, Wang Y. Bolt axial stress measurement based on a mode-converted ultrasound method using an electromagnetic acoustic transducer. Ultrasonics 2014;54:914–20. https://doi.org/10.1016/j.ultras.2013.11.003.
[19] Zhang J, Gu L, Qian X, Ni S, Hou Z. Ultrasonic mearsurement of high strength bolt axial tension in steel construction (in Chinese). Chin J Mech Eng 2006;42:216–20.
[20] Barbosh M, Dunphy K, Sadhu A. Acoustic emission-based damage localization using wavelet-assisted deep learning. J Infrastruct Preserv Resil 2022;3:6. https://doi.org/10.1186/s43065-022-00051-8.
[21] Ramasso E, Verdin B, Chevallier G. Monitoring a bolted vibrating structure using multiple acoustic emission sensors: a benchmark. Data 2022;7:31. https://doi.org/10.3390/data7030031.
[22] Zhang Z, Xiao Y, Su Z, Pan Y. Continuous monitoring of tightening condition of single-lap bolted composite joints using intrinsic mode functions of acoustic emission signals: a proof-of-concept study. Struct Health Monit- Int J 2019;18: 1219–34. https://doi.org/10.1177/1475921718790768.
[23] Zhuo D, Cao H. Damage identification of bolt connections based on wavelet time-frequency diagrams and lightweight convolutional neural networks (in Chinese). Eng Mech 2021;38:228–38.
[24] Wang F, Song G. Looseness detection in cup-lock scaffolds using percussion-based method. Autom Constr 2020;118:103266. https://doi.org/10.1016/j.autcon.2020.103266.
[25] Wang F, Song G, Mo Y-L. Shear loading detection of through bolts in bridge structures using a percussion-based one-dimensional memory-augmented convolutional neural network. Comput-Aided Civ Infrastruct Eng 2021;36: 289–301. https://doi.org/10.1111/mice.12602.
[26] Nguyen T-T, Tuong Vy Phan T, Ho D-D, Man Singh Pradhan A, Huynh T-C. Deep learning-based autonomous damage-sensitive feature extraction for impedance-based prestress monitoring. Eng Struct 2022;259:114172. https://doi.org/10.1016/j.engstruct.2022.114172.
[27] Madhusudana C.K., Kumar H., Narendranath S. Fault Diagnosis of Face Milling Tool using Decision Tree and Sound Signal. Mater. Today-Proc., vol. 5, Amsterdam: Elsevier Science Bv; 2018, p. 12035–12044. https://doi.org/10.1016/j.matpr.2018.02.178.
[28] Li D, Wang Y, Yan W-J, Ren W-X. Acoustic emission wave classification for rail crack monitoring based on synchrosqueezed wavelet transform and multi-branch convolutional neural network. Struct Health Monit- Int J 2021;20:1563–82. https://doi.org/10.1177/1475921720922797.
[29] Li X-X, Li D, Ren W-X, Zhang J-S. Loosening identification of multi-bolt connections based on wavelet transform and resnet-50 convolutional neural network. Sensors 2022;22:6825. https://doi.org/10.3390/s22186825.
[30] Zhang H, Liu B. The recognition of flange bolt connection state based on deep learning (in Chinese). J Appl Acoust 2021;40:350–7.
[31] Hong JC, Sun KH, Kim YY. Dispersion-based short-time Fourier transform applied to dispersive wave analysis. J Acoust Soc Am 2005;117:2949–60. https://doi.org/10.1121/1.1893265.
[32] Zheng X. Looseness Monitoring and Evaluation of Bolt Group Joints in Steel Structure Based on Ultrasonic Guided Waves. Dalian University of Technology; 2018.
[33] Ali L, Alnajjar F, Jassmi HA, Gocho M, Khan W, Serhani MA. Performance evaluation of deep CNN-based crack detection and localization techniques for concrete structures. Sensors 2021;21:1688. https://doi.org/10.3390/s21051688.
[34] Gao X, Wang W. Bolt load looseness measurement for slip-critical blind bolt by ultrasonic technique: a feasibility study with calibration and experimental verification. Struct Health Monit 2023;14759217231173872. https://doi.org/10.1177/14759217231173873.
[35] Chinese National Code. GB/T 3632–2008. Sets of torshear type high strength bolt hexagon nut and plain washer for steel structures, Beijing, China: 2008.
[36] Gao X, Wang W, Teh LH, Zhuang L. A novel slip-critical blind bolt: experimental studies on shear, tensile and combined tensile–shear resistances. Thin-Walled Struct 2022;170:108630. https://doi.org/10.1016/j.tws.2021.108630.
[37] Zhang Y, Xing K, Bai R, Sun D, Meng Z. An enhanced convolutional neural network for bearing fault diagnosis based on time-frequency image. Measurement 2020; 157:107667. https://doi.org/10.1016/j.measurement.2020.107667.
[38] Geron A. Hands-on Machine Learning with Scikit-Learn, Keras, and TensorFlow: Concepts, Tools, and Techniques to Build Intelligent Systems. 2 edition. USA; 2019.